Aeroacoustics research in Europe
The CEAS-ASC report on 2023 highlights

Casalino, Damiano; Schram, Christophe

DOI
10.1016/j.jsv.2024.118732
Publication date
2025
Document Version
Final published version
Published in
Journal of Sound and Vibration

Citation (APA)
Casalino, D., & Schram, C. (2025). Aeroacoustics research in Europe: The CEAS-ASC report on 2023 highlights. *Journal of Sound and Vibration*, *596*, Article 118732. https://doi.org/10.1016/j.jsv.2024.118732

Important note
To cite this publication, please use the final published version (if applicable).
Please check the document version above.

Journal of Sound and Vibration 596 (2025) 118732

Contents lists available at ScienceDirect

Journal of Sound and Vibration

journal homepage: www.elsevier.com/locate/jsvi

Aeroacoustics research in Europe: The CEAS-ASC report on 2023 highlights

Damiano Casalino [a,*], Christophe Schram [b]

[a] Flow Physics and Technology Department, Faculty of Aerospace Engineering, Delft University of Technology, Kluyverweg 1, Delft, 2629 HS, The Netherlands

[b] Environmental and Applied Fluid Dynamics, von Karman Institute for Fluid Dynamics, 72 chausséee de Waterloo, Rhode-St-Genèse, 1640, Belgium

ARTICLE INFO

Keywords:
CEAS Aeroacoustics Specialists Committee
Airframe noise
Propeller noise
Fan noise
Jet noise
Acoustic liners
Metamaterials
Experimental aeroacoustic techniques

ABSTRACT

The Council of European Aerospace Societies (CEAS) Aeroacoustics Specialists Committee (ASC) supports and promotes the interests of the scientific and industrial aeroacoustics community on a European scale and European aeronautics activities internationally. In this context, "aeroacoustics" encompasses all aerospace acoustics and related areas. Each year the committee highlights some of the research and development projects in Europe.

This paper is a report on highlights of aeroacoustics research in Europe in 2023, compiled from information provided to the ASC of the CEAS. In addition, during 2023, a number of research programmes involving aeroacoustics were funded by the European Commission. Some of the highlights from these programmes are also summarized in this article, as well as highlights from other projects funded by national governments and industry.

Contributions are gathered in sections by topic, and a section covering relevant European scientific events in 2023 is also included. Enquiries concerning all contributions should be addressed to the authors who are given at the end of each subsection.

1. Airframe noise

1.1. Innovative coatings for reducing flow-induced cylinder noise by altering the sound diffraction

The aerodynamic tonal noise produced by the flow past a cylinder, which is relevant to many engineering applications, can be modelled by a compact quadrupole at the vortex-shedding instability onset position that is scattered by the surface with a dipolar directivity. When the cylinder is coated with a porous material, the intensity of the shed vortices is reduced, determining a downstream shift of the shedding-outbreak location and the related noise sources. Consequently, sound diffraction is less efficient, and noise is mitigated. In a recent study, Zamponi et al. [1] proposed an innovative coating design based on a further enhancement of this effect. Acoustic-beamforming results showed that, once the leeward part of the flow-permeable cover is integrated with inexpensive and light components that make the flow within the porous medium more streamlined, the quadrupolar source associated with the vortex-shedding onset is displaced more downstream, yielding additional noise attenuation of up to 10 dB with respect to a uniform coating. The same noise-control mechanism can also be exploited when these components are connected to the bare cylinder without the porous cover. In this case, the mitigation of overall sound pressure levels is comparable to that produced by the coated configurations due to the lack of high-frequency noise increase induced by the flow-permeable surface. Remarkable

* Corresponding author.
E-mail addresses: d.casalino@tudelft.nl (D. Casalino), christophe.schram@vki.ac.be (C. Schram).

https://doi.org/10.1016/j.jsv.2024.118732
Received 30 March 2024; Received in revised form 20 August 2024; Accepted 6 September 2024
Available online 12 September 2024

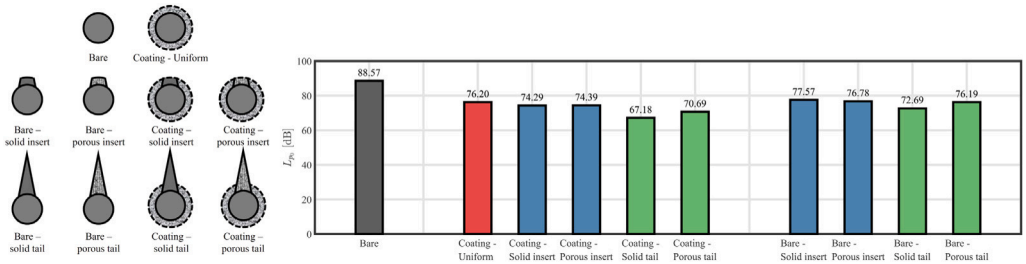

Fig. 1. (a) Overview and nomenclature of the tested configurations based on the bare and coated cylinders. (b) Overall sound pressure level for the different configurations at $Re_d = 4.1 \times 10^4$ integrated between $f = 131.25$ Hz and $f = 20$ kHz.

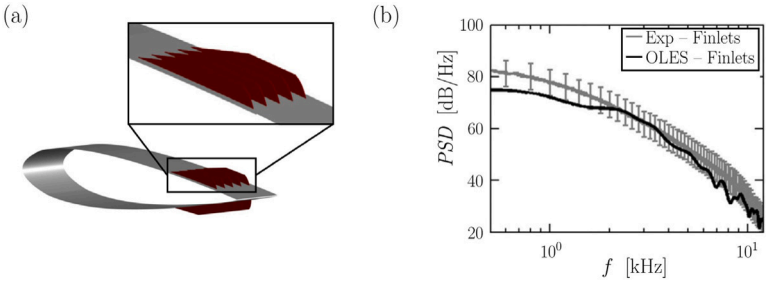

Fig. 2. (a) Schematic showing the finlets mounted near the wing's trailing edge. (b) Power spectral density (PSD) spectrum of surface pressure fluctuations on the suction side near the wing's trailing edge. Experimental data for comparison was provided by Felix Gstrein, University of Bristol (via private communication).

overall-sound-pressure-level reductions of up to 10 dB (see Fig. 1) and potential drag-force decreases are achieved with this approach, which paves the way for disruptive and more optimized noise-attenuation solutions.

1.2. Trailing-edge noise reduction using bio-inspired finlets

Inspired by the fringes present on the feathers of a barn owl, a canopy of streamwise oriented finlets is installed on the aft part of a wing section to investigate its noise reduction mechanisms [2]. Overset-Large Eddy Simulations are carried out, using the CFD/CAA solver viscous-PIANO, of two configurations, (i) the baseline configuration consisting of a wing with a NACA0012 airfoil cross-section, and (ii) an identical configuration, however, now with bio-inspired finlets installed near the trailing edge (see Fig. 2(a)). The chord-based Reynolds number is $\mathrm{Re}_c = 4.2 \times 10^5$ at an angle-of-attack of 4 degrees. The resulting turbulent boundary layer statistics and the power spectral density of the surface pressure fluctuations show good agreement with the experimental data (see Fig. 2(b)). The analysis of the unsteady data revealed various noise reduction mechanisms at play for the considered case. Firstly, finlets 'lift-up' the most energetic eddies in the boundary layer, which prolongs downstream of the finlets (see Fig. 3(a)). As a result of this 'lifting-up' effect, the edge scattering is significantly weakened. Secondly, the finlets mounted on the wing provide an additional wet area to the flow which in-turn has a dissipating effect on the surface pressure fluctuations, thereby again weakening the edge scattering phenomena. However, this also results in an aerodynamic penalty, i.e., an increased drag coefficient. Reduced flow velocities are observed for the flow exiting the finlets channel and towards the trailing edge, which also has a favourable effect in reducing the trailing-edge noise. Finally, in Fig. 3(b) a breakdown of the spanwise coherent length scale for frequencies between 2.5 kHz to 9 kHz is also observed. This study revealed that the finlets mounted upstream of the trailing edge can be effective in reducing the trailing-edge noise, which is a significant contributor to the airframe and wind turbine noise.

Written by Varun B. Ananthan: v.bharadwaj-ananthan@tu-braunschweig.de, TU Braunschweig, Germany, R. A. D. Akkermans, Hamburg University of Applied Sciences, Germany.

1.3. Noise reduction by localized application of porous material to a trailing edge of a circulation-controlled wing

Circulation-controlled wings offer an impressive increase in lift by almost completely avoiding flow separation through the utilization of the Coanda effect, e.g., of the strongly deflected flow on a wing's flap. This contribution reports on a combined aerodynamic and aeroacoustic investigation [3] of local application of porous material to the latter part of the Coanda-jet equipped flap (see Fig. 4(a)). High-fidelity Overset-LES is performed, using the CFD/CAA solver viscous-PIANO, where the porous material is modelled by a volume-averaged approach at a chord based Reynolds number Re_c of 10^6. The application of porous material resulted in enhanced flow through the porous medium, which in-turn thickens the turbulent boundary layer on the flap's suction

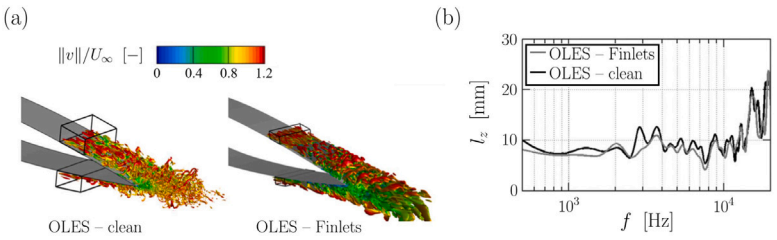

Fig. 3. (a) Iso-surfaces of the Q-criterion coloured with the instantaneous velocity magnitude for the clean and finlet configurations. (b) Overset-LES computed coherent length scale l_z for both the clean and finlet configurations (on the suction side of the at $x/c=0.99$).

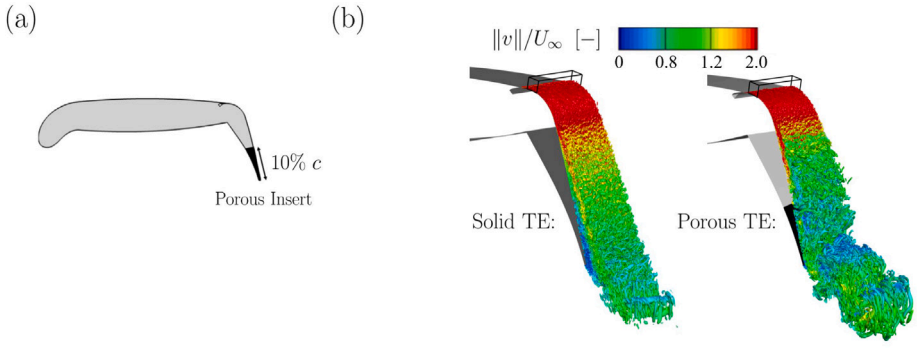

Fig. 4. (a) Schematic of the Coanda-jet equipped flap (flap deflection angle is 65 degrees) with a porous trailing-edge. (b) Iso-surface of the Q-criterion coloured with velocity magnitude.

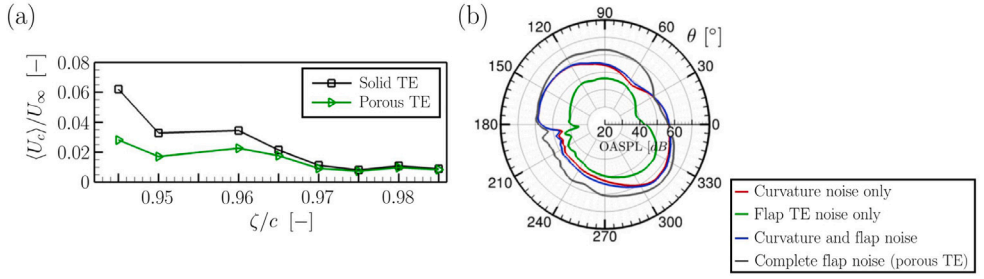

Fig. 5. Coanda-jet equipped flap: (a) Averaged streamwise convective velocity $\langle U_c \rangle$ of the pressure carrying eddies. (b) Far-field OASPL directivities from various sound sources for the porous flap case.

side (i.e., containing larger eddies) (see Fig. 4(b)). Increased spanwise coherent length scales were observed related to the above mentioned larger eddies, especially at mid-frequency range. The convective velocity of these larger eddies were, however, smaller than that of the solid flap configuration (see Fig. 5(a)), which is beneficial to achieve noise reduction. Furthermore, this study emphasizes on the importance of curvature noise and the noise related to the large spanwise vortices, both need to be the focal point of noise reduction studies on such circulation-controlled wings. A source ranking is performed of the different sources of a porous jet-blown flap (e.g., curvature noise and flap trailing-edge noise) (see Fig. 5(b)). The far-field sound characteristics revealed that the noise reduction effect of the porous material is evident for frequencies between 500 and 10 kHz in the forward-downward radiation direction. To conclude, this study provides novel insights regarding the importance of the flow-through aspect of porous material and the subsequent boundary layer thickening and argues that this phenomenon needs to be addressed to achieve a reduction in noise while considering such high-lift generating configurations.

Written by Rinie A.D. Akkermans: rinie.akkermans@haw-hamburg.de, Hamburg University of Applied Sciences, Germany, V. B. Ananthan, TU Braunschweig, Germany, T. Hu, P. Q. Liu, Beihang University, China, D. Burzynski, Coldsense Technologies GmbH, Germany.

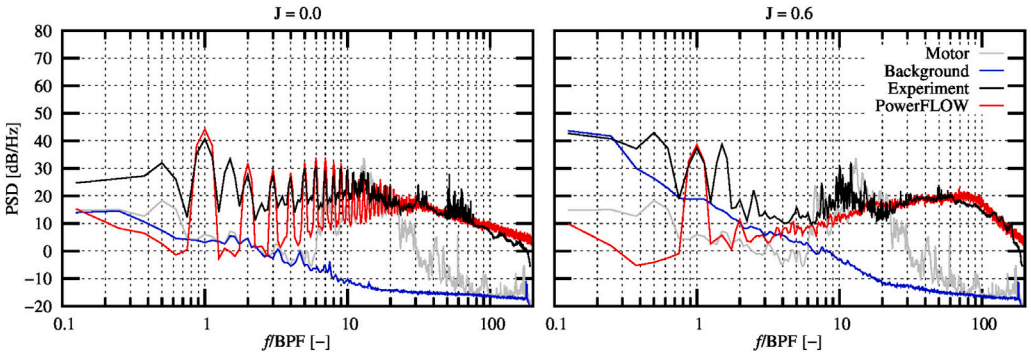

Fig. 6. Rotor far-field noise spectra in hover condition (left) and at advance ration of 0.6 (right). Comparison between measurements (black) and PowerFLOW prediction (red). (For interpretation of the references to colour in this figure legend, the reader is referred to the web version of this article.)

2. Propeller noise

2.1. Flow confinement effects on low-Reynolds number rotor noise

Scale-resolving Lattice-Boltzmann simulations [4] were conducted to investigate the effects of the flow confinement on the noise generated by a drone rotor operating at a low-Reynolds number. A novel version of the VLES turbulence modelling of the commercial solver PowerFLOW was used. The numerical results for a rotor in a pristine flow, both in hover and axial flow conditions, were compared to the results obtained by simulating the rotor in a confined environment reproducing the A-Tunnel anechoic chamber of the TU Delft.

The work confirmed the improved predictive capabilities of the new version of the LB/VLES solver, which provided very accurate far-field noise results in both hover and high advance ratio conditions, including the prediction of the high frequency broadband noise hump related to the presence of a laminar separation bubble, as shown in Fig. 6. Moreover, the new numerical simulation results revealed that, in hover conditions, the dominant effect of the flow recirculation was to increase the unsteady loading tonal noise, contrary to axial flow conditions, where no significant effect due to the test environment was observed.

A noise source identification technique based on the Ffowcs Williams and Hawkings' equation was also presented for the first time. The FWH-based analysis pointed out the impingement of large coherent vortices onto the blade leading-edge as the main source of unsteady loading noise in hover. Moreover, it also identified the scattering of the turbulent boundary-layer pressure fluctuations at the trailing-edge as the primary broadband noise source, along with a secondary radiation mechanism associated to leading-edge turbulence impingement. Conversely, the flow separation and consequent onset of Kelvin–Helmholtz instabilities scattered by the trailing-edge was found to be the main source of broadband noise in axial flow conditions.

Written by Gianluca Romani: gianluca.romani@3ds.com, Dassault Systemes Deutschland GmbH, Germany

2.2. A minimum objective function trim procedure for VTOL noise reduction

The evolution of mobility from two to three dimensions by introducing fully electric vertical take-off and landing vehicles may represent an energy-efficient, safer, and quieter mode of transportation, able to overcome the limited capacity of ground transport. Despite its potentialities, to make urban air mobility aviation a concrete scenario, some unresolved issues must be addressed, among them the mitigation of the acoustic nuisance. To achieve this, different approaches have been proposed, which generally involve suitable design of the vehicle such to minimize the emitted noise. An alternative approach has been proposed in [5], which presents the great advantage of being applicable as an easy retrofitting of already existing vehicles without involving costly redesign.

The idea is to take full advantage of the control redundancy typical of multi-rotor systems by defining the control settings that guarantee the desired steady-state flight conditions while optimizing selected target functions. To this aim, the trim problem is recast into a constrained cost function minimization problem [6]. In principle, the objective function can be arbitrary, vehicle performance, handling qualities, or noise emissions. For instance, in [6], focused on the aerodynamic performance optimization, the numerical results show how a suitable choice of the control settings can effectively reduce the control effort or the hub torque, accordingly to the objective function considered. Then, in [5], an acoustic metric has been included as the objective function, evaluated by suitably coupling the trim solver with an aeroacoustic tool based on the chordwise-compact form of the Farassat 1A formulation for the evaluation of noise radiation. The numerical investigations performed on several multirotor configurations at different operative conditions have demonstrated the capability of the proposed approach to achieve a significant reduction of the emitted noise.

Written by Caterina Poggi, Massimo Gennaretti and Giovanni Bernardini: caterina.poggi@uniroma3.it, Roma Tre University, Italy.

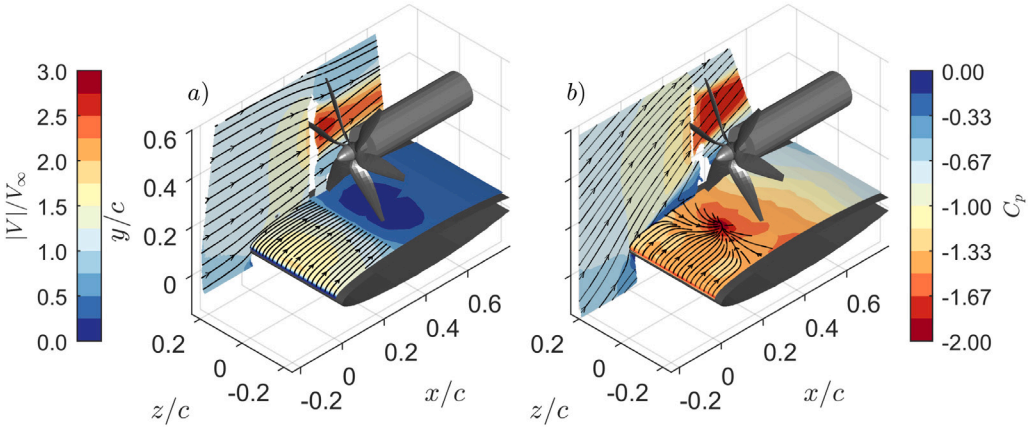

Fig. 7. Experimental pressure coefficient C_p contours over the wing's surface, normalized velocity magnitude $|V|/V_\infty$ contour and 2D velocity streamlines for $J=0.3$ (a) $\alpha=0°$, (b) $\alpha=12°$.

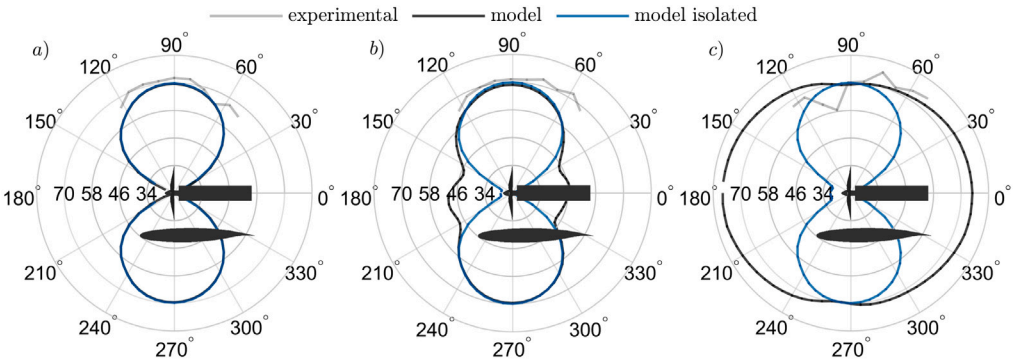

Fig. 8. Experimental and modelled $OASPL$ directivity patterns of the installed rotor for $J=0.6$, in which (a) $\alpha=0°$, (b) $\alpha=8°$ and (c) $\alpha=12°$.

2.3. Aerodynamic noise sources of over-the-wing rotors

Electric Vertical Take-off and Landing (eVTOL) vehicles typically use small-scaled, fixed-pitch rotors, that are operated in proximity of aerodynamic surfaces such as wings and pylons. An example of such a configuration is over-the-wing propulsion. This rotor orientation promises a reduced acoustic footprint during fly-overs, due to the wing's shielding. Nonetheless, the aerodynamic effect of the wing creates complex interactions at the inflow of the rotor, as shown in Fig. 7a and Fig. 7b, leading to additional noise sources [7]. Such aerodynamic noise sources are investigated by aeroacoustic measurements and a low-fidelity model. The model makes use of an analytic description of the inviscid velocity increase by wing's circulation and the ingestion of the separated boundary layer at large angles of attack. This generated inflow serves as an input to an aeroacoustic chain that computes the unsteady loading on the blades and the tonal noise in the far field by helicoidal surface theory. The results show good agreement between the model predictions and experimental data (see Fig. 8). The noise increase by unsteady loading is shown to be sensitive to the angle of attack and is primarily radiated in upstream and downstream directions. By using the low-order model, the effect of the rotor's and wing's geometric and performance parameters can efficiently be analysed. Hence, the conclusions drawn in this research are valuable for the generation of design guidelines for these integrated propulsion systems.

Written by Hasse N.J. Dekker and Daniele Ragni: hasse.dekker@nlr.nl, Wind energy, Faculty of Aerospace Engineering, TU Delft, the Netherland, M. Tuinstra, Vertical Flight and Aeroacoustics department, NLR, the Netherlands

2.4. Lattice Boltzmann method with local wall-refinement for aeroacoustic applications

The Lattice Boltzmann Method (LBM) has been applied in various areas. However, its application to industrially relevant cases leads to high computational costs. This is because with a uniform Cartesian mesh it is not possible to refine the mesh in the wall-normal direction only, thus resulting in high numbers of degrees of freedom for reasonably low y^+ values. A new hybrid grid refinement method was proposed [8], which consists in a reconstruction algorithm in refined near-wall regions, and an in-domain interpolation multi-grid method to improve the accuracy at the interface between different resolution regions. Using this

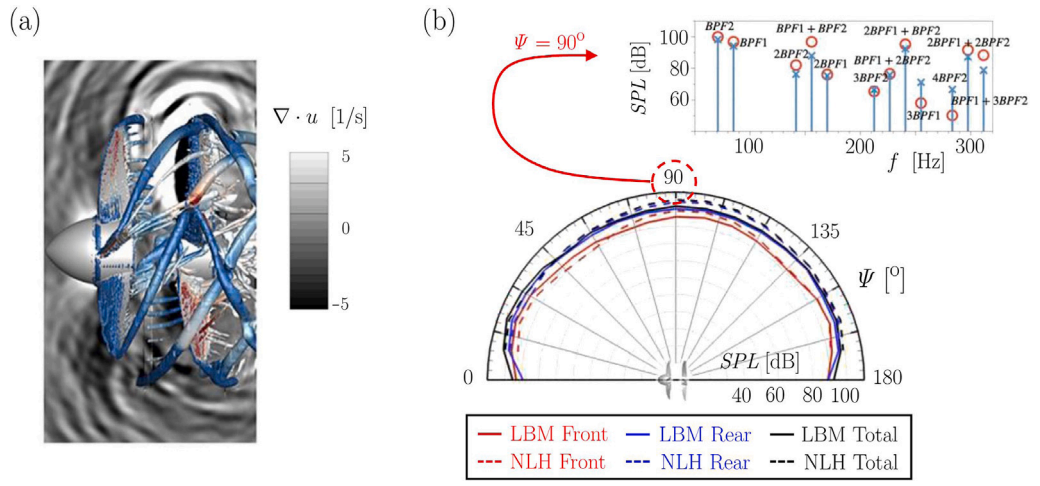

Fig. 9. (a) Instantaneous dilatation $\nabla \cdot u$ contours in the meridian plane and iso-surfaces of Q-criterion. (b) Comparison between LBM and NLH far-field SPL prediction. The insert displays SPL peaks predicted using NLH (circles) and LBM (crosses) methods.

method, the noise generated by counter-rotating propellers (CRPs) was simulated, using the open-source LBM solver Palabos, version 2.0, and compared with the results obtained using the Nonlinear Harmonic (NLH) method available in the commercial software Numeca/FineTurbo. A 6×5 blades CRP configuration is considered at typical take-off condition with flight Mach number $M = 0.21$.

Fig. 9(a) shows contour levels of the velocity dilatation $\nabla \cdot u$ in a meridian plane, with blade-tip and wake vortices visualized as iso-surfaces of Q-criterion. The overall sound pressure level directivities at a distance of 10 rotor diameters are compared in Fig. 9(b). Although the noise levels predicted by the LBM and NLH methods do not fully match at all radiation angles, the overall trends are very similar. Differences between the two methods for the dominant tonal components are less than 2 dB, thus confirming that the proposed LBM approach is in good quantitative agreement with the commercial software.

Written by Changhao Lyu: c.lyu@tu-braunschweig.de, TU Braunschweig, Germany, T. Hu, Beihang University, China, R.A.D. Akkermans, Hamburg University of Applied Sciences, Germany.

3. Fan and jet noise

3.1. Extensive high-resolution measurement of mode-frequency scattering at a fan stage

For the development of low-noise fan designs, rotor shielding and mode-frequency scattering at the rotor have to be considered already in the pre-design phase. In this context specific experimental data is needed for the validation of sound transmission models. However, there is a lack of highly resolved experimental data for model validation that feature isolated propagation effects. To this end, a specifically developed experimental setup has been used to determine the transmission, reflection and scattering characteristics of a fan stage for individually generated modes [9]. By means of a speaker array at the outlet section and microphone arrays installed up- and downstream of the fan stage, as shown in Fig. 10(a), highly resolved measurement data was obtained. A large dataset was generated comprising measurements at two rotor speeds and three flow coefficients and a wide variation of frequencies and mode orders. In particular, the experimental setup enables the detailed evaluation of rotor shielding and mode-frequency scattering for the first time. Exemplary results are given in Fig. 10(b). Rotor co-rotating modes (negative azimuthal orders due to rotor rotation in negative direction) transmit strongly through the fan stage. Rotor shielding affects rotor counter-rotating modes (positive azimuthal mode orders) and leads to a reduction of transmitted sound power by up to 20 dB. The onset of rotor shielding is linked to the scattering mode orders, shown by hollow markers, turning cut-on at the scattering frequency. Mode-frequency scattering causes a shift of sound power in frequency and mode order, typically from a rotor counter-rotating to a co-rotating mode order that transmits efficiently to the inlet and thereby circumvents the blockage effect. Beyond gaining a better physical understanding, the measurement database will be used for the validation of an analytical sound transmission model that is applied in the preliminary fan design process.

Written by Maximilian Behn and Ulf Tapken: maximilian.behn@dlr.de, DLR, Germany

3.2. Data-driven multi-objective optimization of wave-packets for near-field subsonic jet noise

A multi-objective optimization of the shape parameters of a wave-packet is presented in Palma et al. [10], minimizing the prediction error in the jet near-field. The final aim of the work is to develop a jet noise source model able to predict the scattering

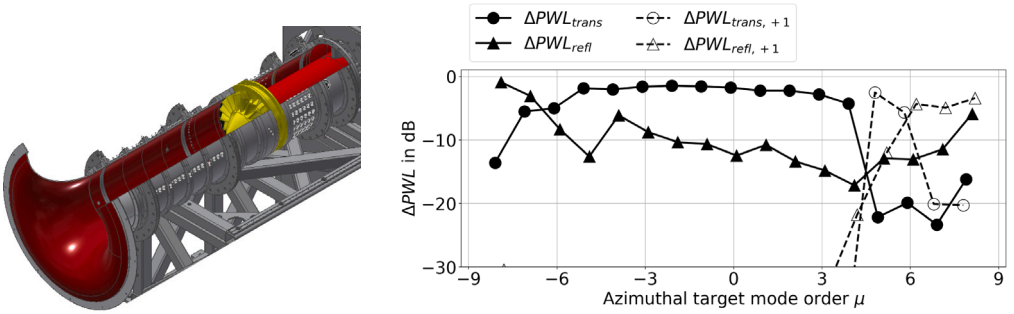

(a) CRAFT fan test rig equipped with (from up- to downstream): inlet microphone array, fan stage, outlet microphone, and speaker array. An inflow control device (not shown) and a bell-mouth inlet ensure a clean base flow.

(b) Level differences of reflected, transmitted and scattered modes at EO 32.5 for a rotor speed of 4500 RPM. Filled markers indicate results at the excitation frequency and hollow markers at the scattering frequency.

Fig. 10. CRAFT rig and results.

effects in closely coupled installed jet configurations, where the flow grazes the scattering surfaces and the hydrodynamic part of the perturbation is relevant. The results are found to provide a good agreement between the numerical reference data and the model in the tested range $0.25 \leq St_D \leq 1$, where the 0th mode is known to be an essential component in the whole jet pressure field, and for radial distances relevant for the jet-surface scattering phenomena in innovative aircraft configurations. A multi-objective optimization procedure aims at matching the complete pressure fluctuation envelope from the model with the one from LES numerical simulations for three radial distances from the jet axis, namely $r/D = 1$, 2, and 2.5, defining the optimal wave-packet parameters. A Pareto front has been obtained as a solution for each optimization due to partially conflicting objectives. The preferred solution on the front is then selected using a Pareto ranking criterion method, considering the wave-packet prediction over an extra line. The optimized noise source model prediction can reproduce the LES data from the free jet with a mean error on each line within 3 dB for most cases. The good prediction at higher radial distances than used in the optimization shows that the model captures some of the features of the noise source, such as the relative contributions of the radiating and non radiating parts of the pressure perturbations. The method is, in principle, applicable to any noise signal produced by jets in which the contribution from coherent structures is significant, and also experimental data is eligible for training the model.

Written by Stefano Meloni: stefano.meloni@unitus.it, University of Tuscia, 01100 Viterbo, VT, Italy, Giorgio Palma, Roma Tre University, Roma, Italy

3.3. High fidelity simulation of isolated and installed jet noise

In the frame of the European Project DJINN (European Union's Horizon 2020 research and innovation Programme, grant agreement No 861438), ONERA developed and validated an advanced High-Fidelity CFD approach for jet noise prediction. It relies on unstructured meshes adapted to the jet flow topology (with standard 2nd order Finite Volume schemes) and a turbulence modelling strategy combining Wall-Modelled LES (ZDES mode 3) and standard RANS/LES (ZDES mode 2). This methodology was first applied to a single stream isothermal jet. Mesh sensitivity and statistical convergence were investigated for the isolated jet at Mach number of 0.9, yielding an agreement between the simulations and the experiments up to St = 10 within 1 dB accuracy for all angles of observation (see Fig. 11). Additional simulations of the installed jet were performed varying the Mach number and plate position to verify the robustness of the approach and to extend the noise radiation methodology developed for isolated configurations to the presence of the wing [11].

Written by Maxime Huet, Fulvio Sartor, Thomas Renaud and Fabien Gand: maxime.huet@onera.fr, ONERA, France.

4. Liners and metamaterials

4.1. Evaluating an additive-manufactured acoustic metamaterial as a nacelle liner using the advanced noise control fan rig

The performance of a 3D-printed acoustic metamaterial as an acoustic treatment for aircraft engine nacelles in the Advanced Noise Control Fan (ANCF) rig has been examined [12].

UHBR engine designs require sound-absorbing liners to be thinner, shorter, and absorb lower-frequency noise. 3D printing can facilitate the manufacture of complex designs which have the potential to be more absorption efficient. Aviation accounted for

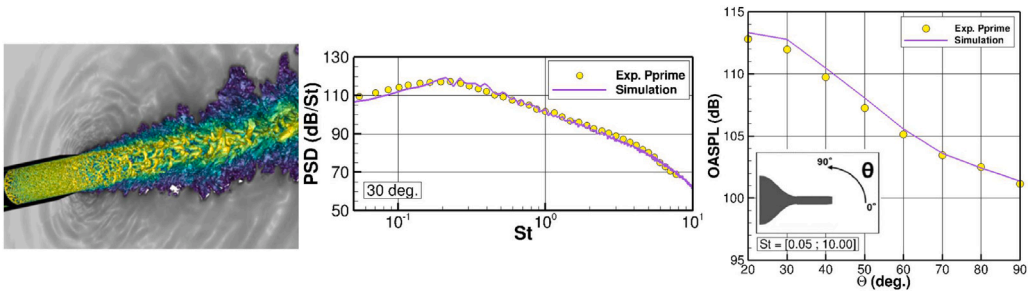

Fig. 11. Illustration of isolated single-stream jet results. From left to right: (a) flow visualization; (b) far-field noise spectra; (c) far-field noise levels. • Measurements by Pprime, — numerical simulation.

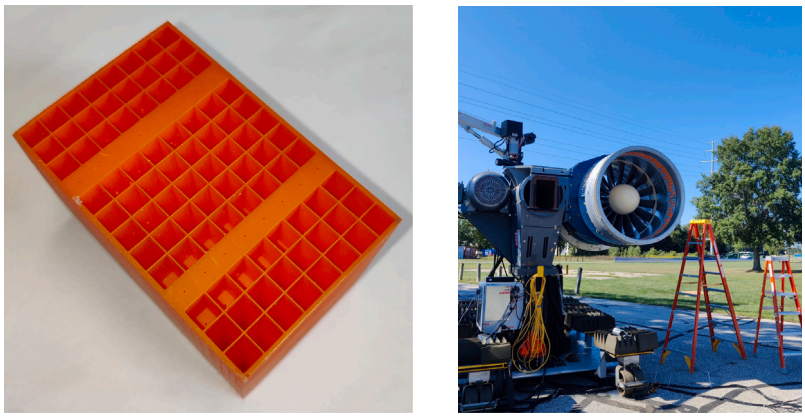

(a) Bottom view of the T-Liner design with integrated faceplate.

(b) T-Liner installed in ANCF at the University of Notre Dame.

Fig. 12. MSLA 3D printed T-Liner.

18.2% of the global additive manufacture (AM) market share in 2017 and it is estimated that the aerospace AM market will exceed $31.8B by 2030. AM can reduce material waste and allow large numbers of components to be consolidated into a single part. An advanced MDOF (AMDOF) liner was designed and 3D printed with a thermosensitive resin using Masked Stereolithography (MSLA) as single part with an integrated faceplate (see Fig. 12). The AMDOF absorber, referred to as the "T-Liner" was 3D printed into 237 blocks of 50 mm depth (2 inch) and inserted into the inlet casing of the ANCF to form an inlet sound-absorbing liner targeting noise at approximately 1 kHz. It was found that the material is capable of reducing the first harmonic of the blade passing frequency, which is the nearest tone to 1 kHz, by up to 18.5 dB, with an overall noise reduction of 3.7 dB (see Fig. 13 as an example result). Future developments will see novel optimization approaches used in a grazing flow situation and 3D printing in metals will be explored.

Written by Gar Bennett: gareth.bennett@tcd.ie, Trinity College Dublin, the University of Dublin, Ireland

4.2. Ultra-broadband sound absorption in a compact multi-chamber micro-perforated panel absorber with varying depths

An optimized, multi-chamber, micro-perforated panel absorber (MC-MPPA) with micro-perforated adjoining panels and varying sub-chamber depths was developed, which can provide a viable, robust aeroengine liner for low frequency, broadband and tonal noise reduction (see Fig. 14). Traditional micro-perforated panel absorbers are constrained by a limited bandwidth, necessitating impossibly small perforations for optimal low-frequency absorption. An innovative design has been proposed [13] and successively improved [14], which addresses these constraints with a lightweight, compact panel structure that uses varying chamber depths and unique porosity per chamber. This work constitutes a technological breakthrough for optimal acoustic liner design based on a graph-theory method. By using the two-point impedance method (TpIM) based on graph theory, a model for multi-chamber MPPAs, which are coupled with each other in two dimensions through perforated side panels, can be developed [15]. The resulting model lends itself to optimization and thus allows the differing geometric parameters of a tessellated network of chambers to be combined to maximize the sound absorption in a frequency range for a particular total absorber depth. The results have been validated theoretically, numerically, and experimentally using 3D printed absorbers.

Written by Jiayu Wang and Gar Bennett: gareth.bennett@tcd.ie, Trinity College Dublin, the University of Dublin, Ireland

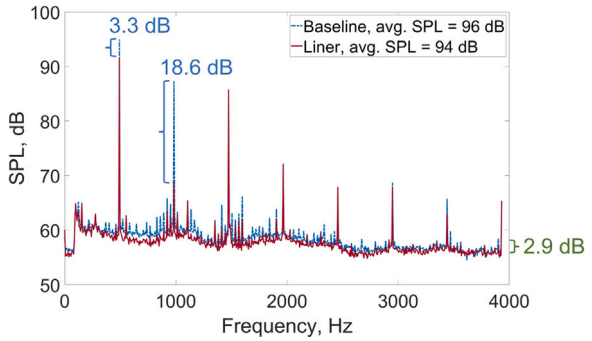

Fig. 13. Spectra at microphone at 43.5° at the nominal speed 1800 RPM. Hardwall versus T-Liner.

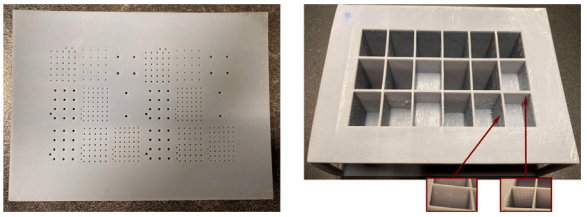

Fig. 14. Photograph of the MC-MPPA an experimental test sample. The top MPP and the core were both 3D printed.

4.3. Spacetime assessment of convective metacontinua response

Acoustic metamaterials designed in quiescent conditions have been shown to suffer significant performance decay when operating in moving media, making their application in aeronautics less effective. Their exotic behaviour is usually achieved by modifying the parameters in the governing equations beyond their natural limits. However, a background flow alters the structure of the wave equation, requiring a redefinition of the metacontinuum constitutive equations. This research aims at extending the static metacontinuum response to convective conditions without the need for a complete redesign. The approach relies on the spacetime reformulation of the governing equations and the application of a spacetime mapping, which recasts the static wave equation into its convective form, preserving the **of the** device. However, since a comprehensive coordinate transformation that fully accounts for convective effects is not known, the introduction of analytical approximations is unavoidable. This requires an assessment of the correction defect and how it impacts the ability of an acoustic metacontinuum to support convective propagation patterns. This work aims to eliminate any artefact arising from the improper spacetime formulation of convective boundary conditions by applying the convective d'Alembertian across a fictitious boundary. In [16], it is proved that any correction defect is due to the spacetime mapping approximation degree: by including the terms neglected by the coordinate change as equivalent sources, in a peculiar acoustic analogy form for the transformed metacontinuum equation, it is possible to obtain the original benchmark represented by the convected d'Alembertian. The unavoidable analytical error leads to a noticeable sensitivity to the relative position of the acoustic source and the device [17] that must be considered. Reducing this effect through the appropriate redistribution of metacontinuum properties is one of the final objectives of this research.

Written by Giada Colombo: giada.colombo@uniroma3.it and Umberto Iemma: umberto.iemma@uniroma3.it, Department of Civil, Computer Science and Aeronautical Technologies Engineering, Roma Tre University, Italy

4.4. Numerical optimization of metasurface cells for acoustic reflection

Palma et al. [18] recently proposed the use of numerical optimization as a strategy to obtain the optimal design parameters of a set of elementary cells for the extension of the frequency range of effectiveness of phase-gradient metasurfaces. The possibility of improving the broadband behaviour of the metasurface is clearly determined and somehow limited by the specific design at hand. In their work, the authors used a space-coiling cell (Fig. 15), but the method applies to any elementary cell type. The broadband design is obtained by minimizing the dependency on the operating frequency of phase delay introduced by the cells, keeping the overall thickness below a quarter of the design wavelength. The optimization approach has been demonstrated to effectively broaden the response of the benchmark metasurface to a 600 Hz–wide frequency range centred on the design frequency of the reference metasurface (Fig. 16). The process can be interpreted as an improvement of the robustness of the design compared to the single-frequency design, obtaining a broadband response not achievable by the reference design.

Written by Lorenzo Burghignoli and Giorgio Palma: lorenzo.burghignoli@uniroma3.it, Roma Tre University, Roma, Italy

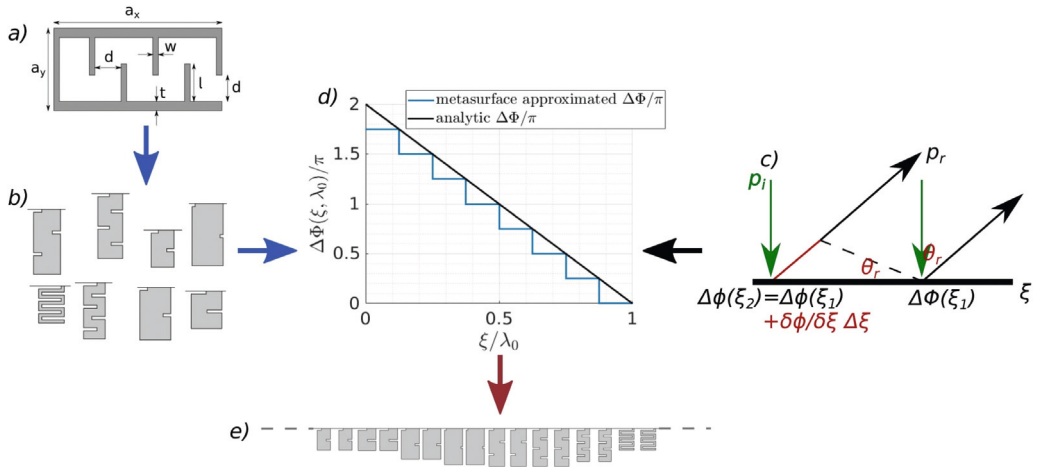

Fig. 15. Illustration of the steps for the design of a phase-gradient-based metasurface. First, the generic cell and its design variables are defined, (a) then, the set of N_c cells composing the building set is created, each one able to introduce a tailored phase shift $\Delta\phi$ in the reflected field, (b) the specific application defines the analytic profile of phase-delay required, (c) the cells in the building set define the stepwise approximation of the desired delay profile, (d), and hence the arrangement of the cells building the metasurface, (e).

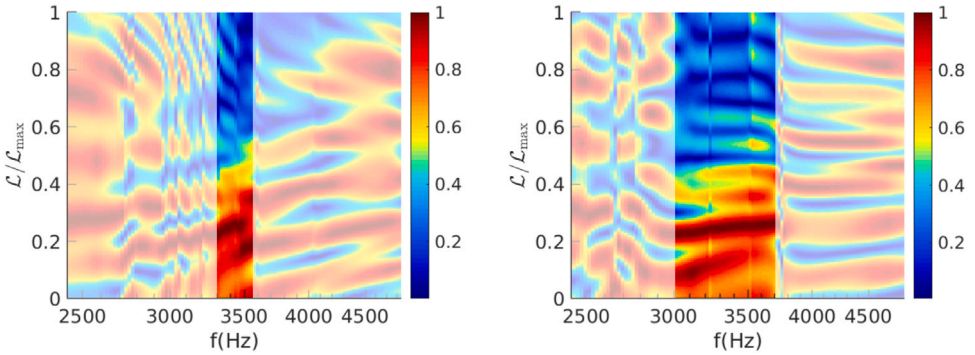

(a) Non-optimized cells (b) Optimized cells

Fig. 16. Absolute value of the reflected acoustic pressure field divided by its maximum evaluated at a line $\mathcal{L}$ distant $\zeta_{\mathcal{L}} = 10\lambda_0$ from the metasurface interface. It can be noted how the optimization widened the effective frequency band of the metasurface: when the extraordinary reflection is happening, the scattered acoustic pressure is focused in the lower part of the picture.

4.5. A metacontinuum model for phase gradient metasurfaces

Acoustic metamaterials and metasurfaces often present complex geometries and microstructures. The development of models of reduced complexity is fundamental to alleviating the computational cost of the analysis. In Palma and Iemma [19] a metacontinuum model for phase gradient-based metasurfaces has been derived and validated. The proposed method unifies the so-called generalized Snell's law and the metacontinuum theory. The metasurface is defined in terms of anisotropic inertia and bulk modulus, whereas thermal and viscous dissipation effects in the metacontinuum are accounted for by introducing a complex-valued speed of sound. A commercial FEM code is used to compare the model prediction with numerical simulations on the original geometry for an exterior acoustics benchmark and an in-duct installation. The metacontinuum model gives solid results for the prediction of the acoustic properties of the examined metasurface samples for all the analysed configurations, as accurate as the equivalent impedance model on which it is based and outperforming it in some circumstances. The model has been tested on space-coiling and Helmholtz resonating cells, however, the bond between the equivalent acoustic impedance of a sample and its metafluid parameters ensures the method's applicability to be wide and general, valid in principle for any design of the acoustic device.

Written by Giorgio Palma: giorgio.palma@uniroma3.it, Roma Tre University, Roma, Italy

4.6. Series and parallel coupling of 3D printed micro-perforated panels and coiled quarter wavelength tubes

Micro-perforated panels (MPPs) and coiled quarter-wavelength resonators (cQWTs) [20] are combined in series and parallel to create a highly tunable multi-resonance system for effective noise suppression (see Fig. 17). The design process involved utilizing

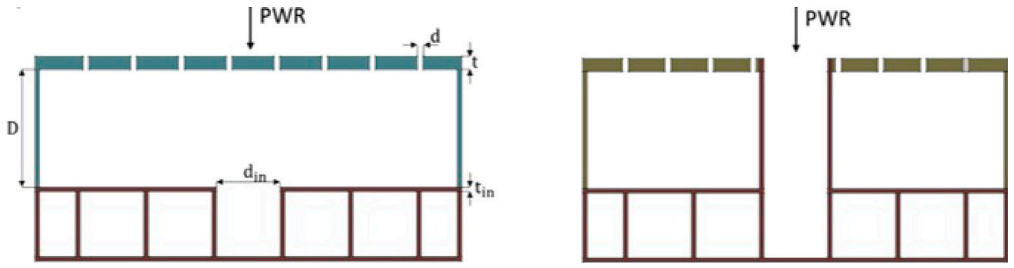

Fig. 17. MPP and coiled Quarted Wavelength Tube (cQWT) in series (left) and in parallel (right).

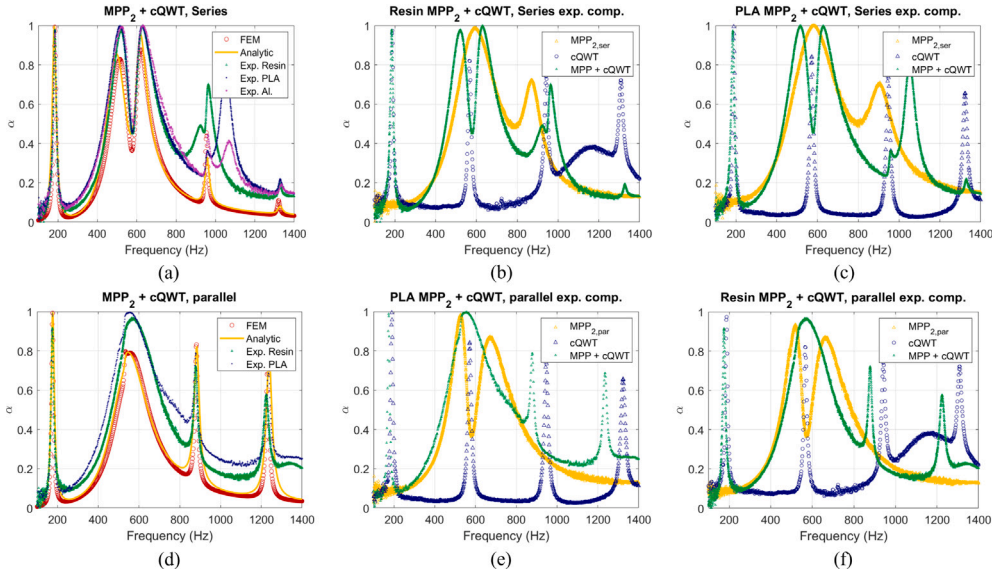

Fig. 18. Sound absorption of MPPs coupled with cQWT in series and in parallel configuration.

Maa's theory for MPPs and the LRF model for cQWTs, while employing an electro-acoustic analogy to determine the total impedance of the hybrid systems. The acoustic sound absorption of these hybrid systems was estimated using numerical simulations and impedance tube experiments [21] on samples made in resin or PLA. The series configuration showed filtering and anti-resonance effects: the cQWT harmonics at higher frequencies of the MPP resonance are suppressed, and when the cQWT peak and MPP are at the same frequency, then anti-resonance appears, resulting in very low sound absorption and the peak splitting in two. On the other hand, the parallel configurations showed superior sound absorption compared to the series case, without anti-resonance and filtering effects (see Fig. 18). Finally, the parallel configuration was tested in two different laboratories using different resin brands, 3D printers, and impedance tubes. The results demonstrated the reproducibility of the samples, thus indicating their potential for implementation in various industrial applications.

5. Experimental techniques in aeroacoustics

5.1. Microphone array measurements on a full aircraft model at high Reynolds numbers in the European Transonic Windtunnel

Noise measurements of a scaled aircraft model at near real-world Reynolds numbers in a pressurized and cryogenic wind tunnel were performed for the first time [22] (see Fig. 19. This study opens avenues for future research, including comparisons between wings and detailed source directivity investigations. It covers the selection of microphones, measurement parameters, array design, and flow parameters, proposing various wind tunnel conditions to distinguish Reynolds and Mach number influences, as well as the impact of slotted versus closed test sections. The data was processed using three-dimensional beamforming with CLEAN-SC deconvolution. Fig. 19(a) shows an image of the model and (b) provides a 3D overview of the estimated sources.

Written by Thomas Ahlefeldt, D. Ernst, A. Goudarzi, H.G. Raumer and C. Spehr: thomas.ahlefeldt@dlr.de, DLR, Germany

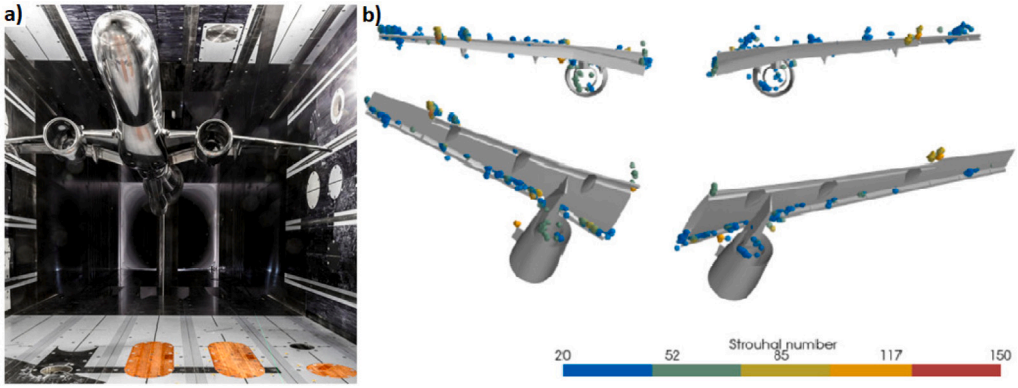

Fig. 19. (a) Photo of model (top) and microphone array (bottom) in the closed test section. b) Overview of dominant sources on the model for Strouhal numbers from 20 to 150 for an exemplary data point.

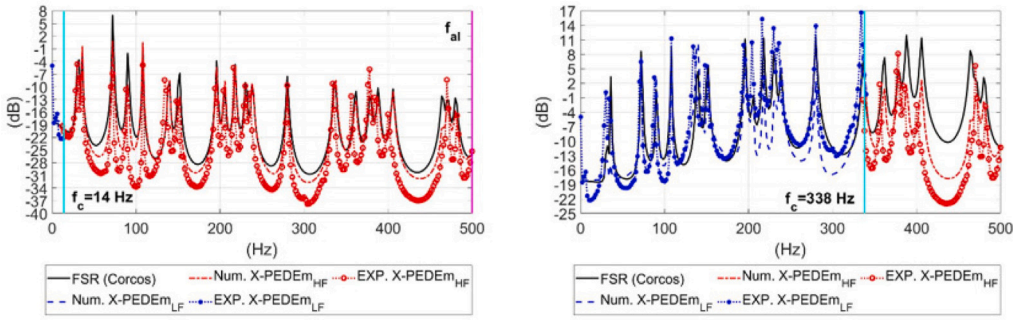

Fig. 20. Panel "A" (all edges free): structural response (PSD acceleration $S_{aa}(\omega)$) to a TBL excitation (Corcos model) at different flow velocities U_0. Comparison between the numerical FSR, numerical X-PEDEM applied in the LF and HF domain, experimental X-PEDEM for the LF and HF domain evaluated for $N_{acq} = 8$ and $N_{ex} = 16$. (a) $U_0 = 25$ m/s, (b) $U_0 = 125$ m/s.

5.2. Evolution of pseudo-equivalent deterministic excitation method for experimental applications

The accurate prediction of vibrational response of a structure under aerodynamic loads is crucial for evaluating initial structural designs and tackling common issues like fatigue and structure-borne sound. Existing literature outlines alternative experimental methods capable of replicating responses to TBL (Turbulent Boundary Layer) excitation without relying on wind tunnel facilities. One such method is the Pseudo-Equivalent Deterministic Excitation method (PEDEM). PEDEM identifies two asymptotic behaviours in the load CSD matrix eigensolutions within the low frequency (LF) and high frequency (HF) domains, avoiding the eigensolutions extraction completely. Previous work has presented the potential of PEDEM for its experimental applications in both HF and LF [23] domains. X-PEDEM, an experimental application of PEDEM, was hence introduced and validated numerically and experimentally through a hammer impact test on three distinct panels under varying boundary conditions and asymptotic flow velocities (example of one panel in Fig. 20). The results obtained from X-PEDEM highlight its capability to approximate reference solutions in various scenarios, ensuring high accuracy for frequencies far away from the convective coincidence frequency (fc). As a result, X-PEDEM emerges as a valuable resource for offering preliminary estimates of vibration levels in structural design. Its experimental configuration proves to be more efficient and straightforward to arrange when compared to a thorough wind tunnel investigation. Furthermore, the post-processing of data demands only a few seconds of computational time, a notable improvement in speed compared to the hours typically necessary for computing a Full Stochastic Response.

Written by Giulia Mazzeo: giulia.mazzeo@ec-lyon.fr, Ecole Centrale de Lyon, France. Giuseppe Petrone, University "Federico II" of Naples, Italy. Sergio De Rosa, University "Federico II" of Naples, Italy. Francesco Franco, University "Federico II" of Naples, Italy. Mohamed Ichchou, Ecole Centrale de Lyon, France. Olivier Bareille, Ecole Centrale de Lyon, France.

5.3. B-CLEAN-SC: CLEAN-SC for broadband sources

The B-CLEAN-SC algorithm was presented [24], a variation of the CLEAN-SC beamforming deconvolution method for broadband sources. Opposed to CLEAN-SC, which deconvolutes the beamforming map for each frequency individually, B-CLEAN-SC processes frequency intervals. Instead of performing a deconvolution iteration at the location of the maximum level, B-CLEAN-SC performs it

at the location of the over-frequency-averaged maximum to improve the location estimation. This averaging cancels out side lobes and achieves super resolution.

Written by Armin Goudarzi: armin.goudarzi@dlr.de, DLR, Germany.

6. Miscellaneous

6.1. Aeroacoustics of micro-slit perforations and broadband noise production by orifices in water cooling systems

Micro-perforated plates are plates with a porosity of a few percent with perforation size of the order of the Stokes layer thickness. This corresponds in the audio range to sub-millimeter or millimeter diameter of perforations. With suitably designed back cavities these plates are very efficient sound absorbers. Manufacturing such small perforations with well defined geometry is a challenge. Slits present the advantage that a single slit can replace tens of circular perforations [25].

Temperature control in nano-meter lithography machines is achieved by means of water cooling through complex pipe circuits. Orifices used to control the flow rate are important sources of sound, which can induce problematic vibrations. The relevant Reynolds number range is around 10^4, based on the pipe diameter and flow velocity. The study explored the possibility of prediction of this noise source based on incompressible Large Eddy Simulations (LES) [26]. The most important result was that for thin orifices the sound sources is almost an order of magnitude lower than for thick orifices. This result obtained experimentally was confirmed by the LES simulations. Similar reduction of the sound source was obtained for the thicker orifices when chamfers were applied both upstream and downstream, leaving a thin central neck of the orifice. Such chamfered orifices are more robust than sharp edged thin orifices.

Written by Avraham Hirschberg: A.Hirschberg@tue.nl, A. Aulitto, S.Kottapalli, G. Nakiboglu, I. Lopez-Arteaga, D.M.J. Smeulders Technische Universiteit Eindhoven, The Netherlands, N. Waterson, ASML, Veldhoven, The Netherlands.

7. Conferences and events

7.1. Fereidoun Farassat memorial symposium

In memory of Fereidoun Farassat, NASA Senior Research Scientist in the field of theoretical aeroacoustics (1944–2011), a Symposium was organized by Delft University of Technology, in collaboration with University Federico II of Naples, Politecnico di Torino and University Roma 3 and, and it was held in Capri, Italy, on 27th-29th September, 2023.[1] The aim of the Symposium was to discuss emerging challenges in aeroacoustics. The event synopsis read:

In the last decade, a profound transformation of the aeroacoustic field has been fostered by the progressive adoption of new experimental and simulation techniques by both academic and industrial players. While some applications have become more mature in the scientific community, other applications are emerging with new theoretical, experimental and numerical challenges.

Experts from industry and academia in several aeroacoustic disciplines were invited to deliver keynote presentations and stimulate panel discussions around current and future challenges of both fundamental and applied nature. As from the program reported in Fig. 21, several topics were covered in sequel sessions, each one followed by technical discussions involving and inspiring experts from all disciplines. Fig. 22 shows group picture of the participants.

7.2. 24th workshop of CEAS-ASC: Aeroacoustics of electrically driven air vehicles: Towards a Green and quiet aviation

The 24th CEAS-ASC Workshop was organized by Budapest University of Technology and Economics and Reziduum Ltd. and took place in Budapest, Hungary, on 12th-13th October, 2023.[2] The aim of this Workshop was to address this issue and to cover many aspects of the aeroacoustics of electrically driven air vehicles. The event synopsis read:

In the last decade, electrically driven vehicles have become widespread on our roads and airspace too. The number of UAVs has increased dramatically, and also the first crewed electric aircraft received its type certificate in 2020. Urban Air Mobility and Advanced Air Mobility are demanding the development of small, highly automated aircrafts to carry passengers and cargo at lower altitudes in and around urban areas. With the increasing number of electrically driven air vehicles, new noise issues are emerging. The Aeroacoustics Specialists Committee of CEAS has decided to address this issue and organize its next workshop on the aeroacoustics of electrically driven air vehicles. The workshop will cover all aspects of electrically driven air vehicles: starting from the physics of noise generation, discussing the sound propagation and its prediction in urban areas, as well as its human effects, on noise annoyance, and covering other topics, such as legislation and noise certification, acoustical measurement, detection and identification techniques.

The event started off with a keynote on EASA's approach to noise regulation of unmanned aircraft in the European Union, given on-line by Guillaume Malaval. Three sessions followed, the first mainly about the assessment and modelling of electric aircraft propulsion. The second session continued with experimental investigations and test rigs and numerical analyses of tilted propellers and broadband noise component, whilst the last session moved to a more virtual domain and had lectures on community noise

[1] https://www.aeroacoustic-symposium.org/

[2] https://www.aircraftnoise.hu

Topic	Speaker	Institution	Country	Title of the keynote
Acoustic Analogy	Jan Delfs	DLR	Germany	Extended use of acoustic integrals for sound propagation and source localization
	Damiano Casalino	3DS	Germany	On truncation effects in FWH
	Mehdi Khorrami	NASA	USA	Simulation-Based Aircraft Noise Certification: Challenges and Opportunities
	Mattia Barbarino	CIRA	Italy	A comprehensive approach based on acoustic analogy for jet noise prediction
	Massimo Gennaretti	Roma 3 Un.	Italy	General Boundary Integral Formulations for Aeroacoustics (and Aerodynamics)
	Ken Brentner	Penn State Un.	USA	Farassat's continuing influence on emerging aeroacoustic problems of practical interest
	Peter Jordan	Poitiers Un.	France	101 uses for a linear operator
Turbomachinery CAA	Julian Winkler	RTX	USA	Emerging Aeroacoustic Challenges for Scale-Resolving Simulations in the Aviation Industry
	Marlene Sanjose	Sherbrooke Un.	Canada	An overview on tip gap noise : simulating noise sources and steps towards modeling
	Cyril Polacsek	ONERA	France	Turbulence-airfoil noise reduction through leading edge serrations: design, prediction methods and advanced applications - Part I
	Martin Buszyk	ONERA	France	Turbulence-airfoil noise reduction through leading edge serrations: design, prediction methods and advanced applications - Part II
	Stephane Moreau	Sherbrooke Un.	Canada	The Third Golden Age of Aeroacoustics
	Julien Christophe	VKI	Belgium	Towards the prediction of wind turbine noise sources in realistic atmospheric flow conditions
Drone/eVTOL rotor aeroacoustics	Christopher Thurman	NASA	USA	Broadband Noise Prediction for Small Hovering Rotors: Discoveries and Observations
	Daniele Ragni	TU-Delft	Netherlands	Aeroacoustic challenges at Low Reynolds Numbers
	Chaitanya Paruchuri	ISVR	UK	Challenges in Mitigating Noise for Advanced Air Mobility Vehicles
	Phil Joseph	ISVR	UK	Recent advances in airfoil noise reduction and new future directions
	Michel Roger	ECL	France	Preliminary Analytical Modeling of the Tonal Noise of Co-Axial Contrarotating Rotors for Drone Propulsion
	Christophe Scharam	VKI	Belgium	An overview of VKI's drone aeroacoustics research
	Bensuhai Lyu	Peking Un.	China	Progress and challenges of modelling, mechanism and control of turbulent boundary layer trailing-edge noise
Acoustic passive treatments	Giorgio Palma	Roma 3 Un.	Italy	Aeroacoustics of metacontinua
	Giuseppe Petrone	Federico II Un.	Italy	Coiled Quarter-Wavelength-Tube Resonators for Low-Frequency Engine Noise Mitigation
	Francesco Avallone	Turin Polytechnic	Italy	On the challenges of determining acoustic impedance in presence of grazing flow
Advanced analysis and measurement techniques	Carsten Spehr	DLR	Germany	Aeroacoustic measurement techniques state of art and where to go
	Roberto Camussi	Roma 3 Un.	Italy	Analysis of an extensive LES database of compressible jets: an experimentalist's approach
	Eduardo Martini	Poitiers Un.	France	Physics of long-ranged resonances using one-way-equations

Fig. 21. Program of the Fereidoun Farassat Memorial Symposium, 27th-29th September, 2023, Capri, Italy.

Fig. 22. Group picture of the Fereidoun Farassat Memorial Symposium, 27th-29th September, 2023, Capri, Italy.

Fig. 23. Group picture of the 24th CEAS-ASC Workshop, 12th-13th October, 2023, Budapest, Hungary.

assessment, and auralization framework, AI based flight path optimization and beamforming based localization techniques. The second day's keynote was presented by Dr. Stephen A. Rizzi (NASA) on Community Noise Impact of Urban Air Mobility Vehicle Operations. The two following sessions covered noise reduction techniques, further analyses of noise generation of small electrical aircraft, and on the optimization of aeroacoustic design. Fig. 23 shows group picture of the participants.

Written by Attila Nagy: anagy@epsz.bme.hu, Budapest University of Technology and Economics, Hungary.

CRediT authorship contribution statement

Damiano Casalino: Writing – original draft, Conceptualization. **Christophe Schram:** Writing – review & editing.

Declaration of competing interest

The authors declare that they have no known competing financial interests or personal relationships that could have appeared to influence the work reported in this paper.

Data availability

No data was used for the research described in the article.

Acknowledgement

The authors are grateful to Gar Bennett of Trinity College Dublin for his kind support on collecting the different contributions.

References

[1] R. Zamponi, D. Ragni, S. Van Der Zwaag, F. Avallone, Innovative coatings for reducing flow-induced cylinder noise by altering the sound diffraction, Phys. Fluids 35 (12) (2023) 127120, http://dx.doi.org/10.1063/5.0177263.
[2] V. Ananthan, R. Akkermans, Trailing-edge noise reduction using bio-inspired finlets, J. Sound Vib. 549 (2023) 117553, http://dx.doi.org/10.1016/j.jsv.2023.117553.
[3] V. Ananthan, R. Akkermans, T.L. Hu, D. P.Q., Effects of localized application of porous material on trailing-edge noise of a circulation-controlled wing, Int. J. Heat Fluid Flow 103 (2023) 109209, http://dx.doi.org/10.1016/j.ijheatfluidflow.2023.109209.
[4] D. Casalino, G. Romani, L.M. Pii, R. Colombo, Flow confinement effects on sUAS rotor noise, Aerosp. Sci. Technol. 143 (2023) 108756, http://dx.doi.org/10.1016/j.ast.2023.108756.
[5] C. Poggi, G. Bernardini, M. Gennaretti, A minimum objective function trim procedure for VTOLs noise reduction, Aerosp. Sci. Technol. 147 (2024) 109004, http://dx.doi.org/10.1016/j.ast.2024.109004.
[6] C. Poggi, G. Bernardini, M. Gennaretti, F. Porcacchia, Optimal performance trim procedure for multirotor vertical takeoff and landing vehicles, J. Aircr. (2023) 1–11, http://dx.doi.org/10.2514/1.C037486.
[7] H.N. Dekker, H. Brouwer, J. Kok, M. Laban, M. Tuinstra, Tonal noise measurements and simulations of an Over-The-Wing propeller, in: AIAA AVIATION 2023 Forum, AIAA, San Diego, California, 2023, http://dx.doi.org/10.2514/6.2023-3358.
[8] C. Lyu, P. Liu, T. Hu, V. Geng, Q. Qu, T. Sun, R. Akkermans, Hybrid method for local-wall refinement in lattice Boltzmann method simulations, Phys. Fluids 35 (2023) 017103, http://dx.doi.org/10.1063/5.0130467.
[9] M. Behn, U. Tapken, Experimental investigation of mode-frequency scattering at fan stages, in: Proceedings of the ASME Turbo Expo 2023: Turbomachinery Technical Conference and Exposition. Volume 13C: Turbomachinery - Deposition, Erosion, Fouling, and Icing Design Methods and CFD Modeling for Turbomachinery Ducts, Noise, and Component Interactions., in: GT2023-101882, ASME, Boston, Massachusetts, 2023, http://dx.doi.org/10.1115/GT2023-101882.
[10] G. Palma, S. Meloni, R. Camussi, U. Iemma, C. Bogey, Data-driven multiobjective optimization of wave-packets for near-field subsonic jet noise, AIAA J. 61 (5) (2023) 2179–2188, http://dx.doi.org/10.2514/1.J062261.
[11] M. Huet, F. Gand, G. Rahier, Simulation of isolated and installed jet noise at mach=0.9: Influence of numerical mesh and physical insights, Flow Turbul. Combust. (2023) http://dx.doi.org/10.1007/s10494-023-00461-y.
[12] E.P. Ross, K.M. Figueroa-Ibrahim, D.L. Sutliff, S. Morris, G.J. Bennett, Evaluation of an additive-manufactured acoustic metamaterial as an Nacelle Liner using the active noise control fan, in: AIAA AVIATION 2023 Forum, American Institute of Aeronautics and Astronautics, San Diego, CA and Online, 2023, http://dx.doi.org/10.2514/6.2023-3827.
[13] J. Wang, G.J. Bennett, Multi-chamber micro-perforated panel absorbers optimised for high amplitude broadband absorption using a two-point impedance method, J. Sound Vib. 547 (2023) 117527, http://dx.doi.org/10.1016/j.jsv.2022.117527.
[14] J. Wang, G.J. Bennett, Ultra-broadband sound absorption in a compact multi-chamber micro-perforated panel absorber with varying depths, AIP Adv. 14 (1) (2024) 015009, http://dx.doi.org/10.1063/5.0187328.
[15] J. Killeen, I. Davis, J. Wang, G.J. Bennett, Fan-noise reduction of data centre telecommunications' server racks, with an acoustic metamaterial broadband, low-frequency sound-absorbing liner, Appl. Acoust. 203 (2023) 109229, http://dx.doi.org/10.1016/j.apacoust.2023.109229.
[16] G. Colombo, G. Palma, L. Burghignoli, U. Iemma, Assessment of the convective correction defect of metacontinua using spurious sources in the aeroacoustic spacetime, in: AIAA AVIATION FORUM, Session: Computational Methods and Techniques in Aeroacoustics, 2023, http://dx.doi.org/10.2514/6.2023-4060.
[17] G. Colombo, G. Palma, L. Burghignoli, U. Iemma, Spacetime acoustic analogy for the assessment of convective correction of metacontinua, in: Proceedings of the 29th International Congress on Sound and Vibration, ICSV, 2023.
[18] G. Palma, F. Centracchio, L. Burghignoli, I. Cioffi, U. Iemma, Numerical optimization of metasurface cells for acoustic reflection, AIAA J. 62 (3) (2024) 1136–1147, http://dx.doi.org/10.2514/1.J063399.
[19] G. Palma, U. Iemma, A metacontinuum model for phase gradient metasurfaces, Sci. Rep. 13 (1) (2023) 13038, http://dx.doi.org/10.1038/s41598-023-39956-z.
[20] G. Catapane, G. Petrone, O. Robin, K. Verdière, Coiled quarter wavelength resonators for low-frequency sound absorption under plane wave and diffuse acoustic field excitations, Appl. Acoust. 209 (2023) 109402, http://dx.doi.org/10.1016/j.apacoust.2023.109402.
[21] G. Catapane, G. Petrone, O. Robin, Series and parallel coupling of 3D printed micro-perforated panels and coiled quarter wavelength tubes, J. Acoust. Soc. Am. 154 (2023) 3027–3040, http://dx.doi.org/10.1121/10.0022378.
[22] T. Ahlefeldt, D. Ernst, A. Goudarzi, H.-G. Raumer, C. Spehr, Aeroacoustic testing on a full aircraft model at high Reynolds numbers in the European transonic windtunnel, J. Sound Vib. 566 (2023) 117926, http://dx.doi.org/10.1016/j.jsv.2023.117926.
[23] G. Mazzeo, G. Petrone, F. Franco, S. De Rosa, M.N. Ichchou, O. Bareille, Experimental pseudo-equivalent deterministic excitation method extension for low frequency domain applications, J. Acoust. Soc. Am. 154 (6) (2023) 3507–3520, http://dx.doi.org/10.1121/10.0022375.
[24] A. Goudarzi, B-CLEAN-SC: CLEAN-SC for broadband sources, JASA Express Lett. 3 (9) (2023) http://dx.doi.org/10.1121/10.0020992.
[25] A. Aulitto, A. Hirschberg, I. Lopez Arteaga, V. Saxena, Experimental study of a slit in the presence of a bias flow under medium- and high-level acoustic excitation, Int. J. Spray Combust. Dyn. 15 (2023) 117–126, http://dx.doi.org/10.1177/17568277231167855.
[26] S. Kottapalli, S. van Aken, A. Hirschberg, N. Waterson, D. Smeulders, G. Nakiboglu, Influence of orifice thickness and chamfer on broadband noise in a water circuit, Acta Acust. 7 (2023) 66, http://dx.doi.org/10.1051/aacus/2023058.